Chemical Science

Accepted Manuscript

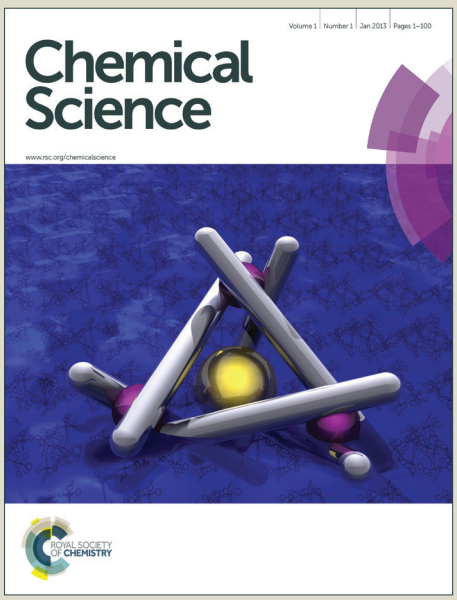

ROYAL SOCIETY OF CHEMISTRY

www.rsc.org/chemicalscience

Journal Name

RSCPublishing

COMMUNICATION

Air-stable ambipolar field-effect transistor based on a solution-processed octanaphthoxy-substituted tris(phthalocyaninato) europium semiconductor with high and balanced carrier mobilities

Cite this: DOI: 10.1039/x0xx00000x

Received 00th January 2012,
Accepted 00th January 2012

DOI: 10.1039/x0xx00000x

www.rsc.org/

Xia Kong,[a] Xia Zhang,[a] Dameng Gao,[a] Dongdong Qi,[b] Yanli Chen*[a] and Jianzhuang Jiang*[b]

Abstract: Simple solvent-vapor annealing over the QLS film-based OFET devices fabricated from (Pc)Eu[Pc(ONh)$_8$]Eu[Pc(ONh)$_8$] led to the high and balanced ambipolar performance that has never been revealed for a small molecule single-component-based solution processed devices, with the mobilities of 1.71 and 1.25 cm^2 V^{-1} s^{-1} for holes and electrons, respectively, under ambient conditions.

Since the first demonstration of the ambipolar charge transport in a bilayer organic thin-film transistor of organic semiconductors,[1] significant progress has been achieved towards their practical applications in the ultra-low-cost, large-area complementary integrated circuits without necessarily requiring micropatterning of the individual *p*- and *n*-channel semiconductors.[2] In particular, for the purpose of understanding the structure-functionality relationship, small molecule-based ambipolar organic semiconductors attracted a wide range of research interests. In 1990 the organic field-effect transistors (OFETs) fabricated from bis(phthalocyaninato) lanthanide compounds (Pc)M(Pc) (M = Tm, Lu) with a narrow band gap were found to show ambipolar characteristics with hole mobility of 10^{-3}~10^{-4} cm^2 V^{-1} s^{-1} and electron mobility of 10^{-4}~10^{-5} cm^2 V^{-1} s^{-1} in vacuum, respectively, revealing the ambipolar nature of the single organic component for the first time.[3] As can be easily expected, this study was followed by extensive investigations with the disclosing of the ambipolar nature for polymers,[4] oligomers,[5] and in particular a series of small molecules including the acene derivatives with a wide band gap, E_{gap}>1.8 eV.[6] Among which the ultrapure rubrene single crystal-based OFET devices appear to present the best result with the hole mobility of 43 cm^2 V^{-1} s^{-1} and electron mobility of 0.81 cm^2 V^{-1} s^{-1} in vacuum despite the still non-balanced mobilities between the two carriers due mainly to the mismatch between the standard electrodes (Au, Ag, or Al) and the LUMO level of rubrene.[7] Modification over the acene-bone via silylethynylation seems to be able to improve the balance, resulting in the hole mobility of 0.22 cm^2 V^{-1} s^{-1} and electron mobility of 1.1 cm^2 V^{-1} s^{-1} also in vacuum for the chemical vapor deposition (CVD) film-based OFET devices fabricated from silylethynylated N-heteropentacene.[8] However, when tested in ambient air, the electron mobility significantly decreased to the range of 10^{-3} cm^2 V^{-1} s^{-1} due to the electron trapping by oxygen or water. To the best of our knowledge, solution processed small molecule-based ambipolar OFETs in particular those with air-stable nature still remain rare, with the best result achieved over the (p-fluoro)phenoxy-substituted tris(phthalocyaninato) europium semiconductor with the hole mobility of 0.24 cm^2 V^{-1} s^{-1} and electron mobility of 0.042 cm^2 V^{-1} s^{-1}.[9] For the purpose of further improving the device performance in particular the balance between the two carrier mobilities, both phthalocyanine and porphyrin ligands were simultaneously fabricated into the tris(tetrapyrrole) metal skeleton.[10] This, however, induced the significant decrease in the charge mobilities despite the effective improvement over the balance between the two carrier mobilities.

On the other hand, solvent-vapor annealing (SVA) method using high boiling-point marginal solvent (instead of good and poor solvent) is well known to be able to effectively increase the molecular ordering and orientation and in turn the crystallinity of a preformed thin film.[11] As a consequence, in recent years this technique has been well employed to improve the OFET performance of solution processed organic semiconductors with single-polar nature. In 2006, by utilizing the SVA technique the hole mobility of triethylsilylethynyl anthradithiophene *p*-type semiconductor was effectively increased from 0.002 cm^2 V^{-1} s^{-1} for the solution-processed film to 0.2 cm^2 V^{-1} s^{-1} for the SVA film.[12] Nevertheless, the mobility for electrons of the 1,2-dichloroethane (DCE)-vapor-annealed devices fabricated from the *n*-type dialkyl-substituted-dicyanoperylene tetracarboxylic diimide derivatives was also effectively improved to a large degree from 0.02 to 0.5 cm^2 V^{-1} s^{-1}.[11] However, to the best of our knowledge, this SVA method has not yet been employed to the small molecule-based ambipolar organic semiconductor-based OFET devices.

In the present paper, we describe the design and preparation of a novel heteroleptic tris(phthalocyaninato) europium complex with unsymmetrical triple-decker molecular structure, (Pc)Eu[Pc(ONh)$_8$]Eu[Pc(ONh)$_8$] (**1**) [Pc = unsubstituted phthalocyanine; Pc(ONh)$_8$ = 2,3,9,10,16,17,23,24-octanaphthoxy phthalocyanine], Scheme 1. Electrochemistry study reveals its potential air stable and balanced ambipolar organic semiconductor

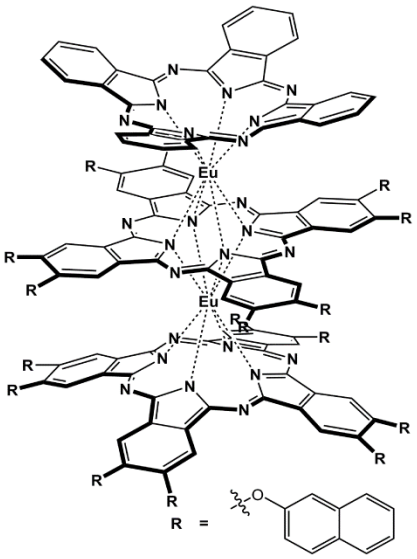

Scheme 1 Schematic molecular structure of tris(phthalocyaninato) europium triple-decker complex (Pc)Eu[Pc(ONh)$_8$]Eu[Pc(ONh)$_8$] (**1**).

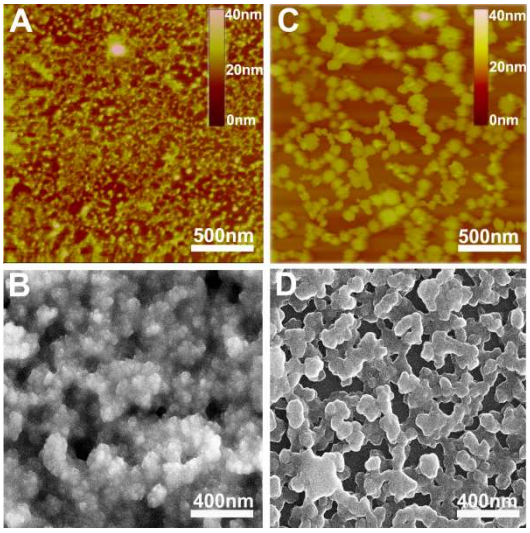

Fig. 1 AFM and SEM images the pristine QLS film (A, B) and SVA film (C, D) of **1**.

nature,[2c] which is indeed verified by the performance, despite not high, of the solution processed quasi–Langmuir–Shäfer (QLS) film-based OFET devices fabricated from this compound. Nevertheless, simple solvent annealing over the QLS films using *o*-dichlorobenzene (DCB) induces significant improvement over the device performance with good on/off ratio of 10^6 and in particular the high and balanced carrier mobilities of 1.71 cm^2 V^{-1} s^{-1} for holes and 1.25 cm^2 V^{-1} s^{-1} for electrons that has never been reported for small molecule single-component-based OFET devices.

Heteroleptic tris(phthalocyaninato) europium triple-decker complex (Pc)Eu[Pc(ONh)$_8$]Eu[Pc(ONh)$_8$] (**1**) was prepared following the published procedures[9,13] and characterized by a series of spectroscopic methods including MALDI-TOF mass and ^{1}H NMR, Figs. S1† and S2†. On the basis of the previous investigation results,[9,10,13] in the present case eight naphthoxy substituents with slight electron-withdrawing nature were introduced onto the periphery of the bottom and medium phthalocyanine ligands in the triple-decker molecule to tune the HOMO and in particular the LUMO energy level towards enhancing the electron transport as well as the air-stability of corresponding organic semiconductor.[14] Nevertheless, the unsymmetrical structure of the target heteroleptic triple-decker compound isolated in combination with the effect of the bulky naphthoxy substituents also ensures its good solubility in common organic solvents and in turn its good solution processability.[13] Most importantly, design and preparation of such a heteroleptic tris(phthalocyaninato) europium compound involving different tetrapyrrole ligands are actually expected to afford ambipolar organic semiconductor with balanced carrier mobility between electrons and holes as mentioned above.[10]

Differential pulse voltammetry (DPV) measurement over (Pc)Eu[Pc(ONh)$_8$]Eu[Pc(ONh)$_8$] (**1**) in CH_2Cl_2 reveals a couple of one-electron redox couples with the first oxidation and first reduction potential at + 0.63 and – 0.44 V (vs. SCE), Fig. S3† and Table S1†. Both the HOMO and LUMO energies at –5.07 and –4.00 eV thus derived for this triple-decker match well with the work function of gold electrode at –5.1 eV and locate in the energy range required for good *p*- and in particular air-stable *n*-type organic semiconductors, respectively, ensuring the simultaneous facilitation of both the hole and electron injections from the Au electrodes. This in turn suggests the potential of this triple-decker compound in air-stable ambipolar OFET devices with good performance.

Ordered multilayers of (Pc)Eu[Pc(ONh)$_8$]Eu[Pc(ONh)$_8$] (**1**) were prepared by a solution-based QLS method.[15] The morphology of the triple-decker QLS film was characterized by atomic force microscopy (AFM) and scanning electron microscopy (SEM), Figs. 1A and 1B. The images show the small domains of approximately 40~60 nm in size with some gaps and cracks between aggregate domains. The out-of-plane (OOP) X-ray diffraction pattern (XRD) of the QLS film in low-angle range exhibits one sharp diffraction peak at 2.19 nm (2θ = 4.05°), Fig. 2A, which corresponds to the thickness of one layer of QLS film, suggesting a layered structure for this QLS film.[16] Polarized UV-vis spectroscopy was employed to detect the orientation (dihedral angle between Pc rings and the surface of substrate) of the Pc rings in the film,[17] revealing the "edge-on" conformation of the triple-decker molecules in the film on the substrate with the dihedral angle of 52.6° and the formation of *J*-aggregates of the triple-decker molecules in the film, Fig. S4A† and Table S2† and insert of Fig. 2A. This is in line with the calculated result based on the simulated triple-decker molecular dimension (2.86 nm, Fig. S5†)[13,18] and the above-mentioned OOP XRD result (2.19 nm), with the orientation angle of 50.0°. Furthermore, the triple-decker (Pc)Eu[Pc(ONh)$_8$]Eu[Pc(ONh)$_8$] (**1**) displays a Q band at 655 nm in $CHCl_3$ solution, Fig. S6†, which red-shifts to 662 nm in QLS film, confirming the formation of *J*-aggregates and indicating the strong interaction between the neighboring molecules.[19]

As exemplified in Fig. S7†, the OFET device fabricated from **1** on a hexamethyldisilazane (HMDS)-treated SiO_2/Si substrate using the QLS technique with a bottom-gate top-contact configuration showed typical ambipolar (both *p*-channel and *n*-channel) characteristics in air. The carrier mobility (μ) was calculated by using the saturation region transistor equation, $I_{ds} = (W/2L)\mu C_0(V_G - V_T)^2$, where I_{ds} is the source-drain current, V_G the gate voltage, C_0 the capacitance per unit area of the dielectric layer, and V_T the threshold voltage.[20] In air, the device presents the carrier mobility for holes of 2.16×10^{-6} cm^2 V^{-1} s^{-1} (V_{ds}, –100 V), Fig. S7A†. Nevertheless, under ambient condition this device simultaneously displays the carrier mobility for electrons of 3.15×10^{-6} cm^2 V^{-1} s^{-1} (V_{ds}, 100 V), Fig. S7B†. These results clearly reveal the air-stable ambipolar nature of OFET device fabricated from the heteroleptic tris(phthalocyaninao) europium compound with balanced carrier mobilities between holes and electrons despite their relatively low values.[9,10,13] In line with this result, the current on/off ratios, locating in the range of *ca.* 10^2 for both the *p*- and *n*-channel transports in the ambipolar OFET device, are also not good for the QLS film-based devices of **1**, Table S3†.

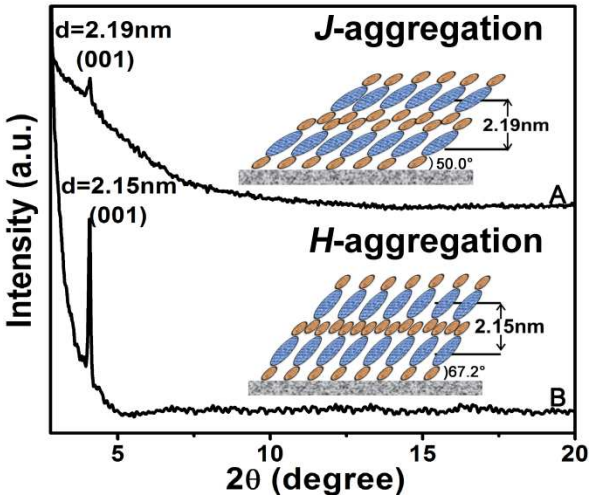

Fig. 2 XRD patterns of the pristine QLS film (A) and SVA film (B) of **1**. The inserts are schematic packing modes of the triple-decker **1** in QLS and SVA film, respectively.

This, however, seems not true for the threshold voltages (V_T) with the value of –16 and +2 V for holes and electrons, respectively, obtained for the QLS film-based OFET device. In comparison with the ambipolar performance of the (Pc)Eu[Pc(OPh)$_8$]Eu[Pc(OPh)$_8$] QLS film-based devices reported previously by this group with the mobilities of 0.68 cm^2 V^{-1} s^{-1} for electrons and 0.014 cm^2 V^{-1} s^{-1} for holes,[13] indeed lower carrier mobilities for both holes and electrons were obtained for the (Pc)Eu[Pc(ONh)$_8$]Eu[Pc(ONh)$_8$] QLS film-based OFETs in the present case. This seems strange at the first glance but could be easily rationalized on the basis of the formation of different aggregates in QLS films with *H*-aggregation mode revealed for (Pc)Eu[Pc(OPh)$_8$]Eu[Pc(OPh)$_8$][13] but *J*-aggregation mode for (Pc)Eu[Pc(ONh)$_8$]Eu[Pc(ONh)$_8$] in the present work on the basis of a series of spectroscopic and in particular XRD analysis results.

To enhance the device performance fabricated from this triple-decker compound, the pristine QLS films of **1** were simply treated by solvent-vapor annealing under an atmosphere saturated with the marginal DCB vapor at 100 °C for 30 min by releasing 20μL of solvent in the Petri dish (diameter: 9.5 cm, height: 1.5 cm, volume: 106.3 cm^3), Fig. S8†, affording the solvent-vapor annealed (SVA) films. The morphology of the triple-decker SVA film was observed by AFM and SEM to show a typical two-dimensional wafer-like structure with more uniform grain crystallites approximately 100~150 nm in diameter and decreased grain boundary compared to those of the pristine QLS film, Figs. 1C and 1D, revealing the highly improved film structure and morphology after the annealing process using DCB solvent due likely to significantly lowering the activation energy for rearrangement in soluble π-conjugated molecules.[11,12] The increase in the grain size and decrease in the grain boundary would be beneficial to the charge transport in such a SVA film relative to its pristine QLS film. The out-of-plane (OOP) XRD pattern in low-angle range of the SVA film exhibits one strong and sharp diffraction peak at 2.15 nm (2θ = 4.10°), Fig. 2B, which corresponds to the thickness of one layer of SVA film, suggesting regular layered structure for this film.[16] Polarized UV-vis spectroscopic technique reveals a slipped co-facial *H*-type stacking mode of the triple-decker molecules in the film on the substrate due to the dihedral angle of 67.2°, Fig. S4B† and Table S2† and insert of Fig. 2B. As a consequence, the *d*-spacing of 2.15 nm in the SVA film revealed by OOP XRD technique does not correspond with that calculated according to the simulated triple-decker molecular dimension (2.86 nm)[13,18] and the polarized UV-vis result (67.2°), 2.64 nm. Such an obvious decrease (*ca.* 18%) of *d*-spacing in the SVA film indeed seems strange at the first glance, which however could be rationalized on the basis of the increased interlayer interaction through effective side naphthoxy-moiety interdigitation between the neighbouring triple-decker molecules in the out-of-plane direction upon DCB vapor annealing.[21] It is noteworthy that the (001) diffraction peak with increased intensity and sharpening in the low-angle region of the SVA film relative to that of the pristine QLS film of **1** clearly indicates the obviously improved molecular ordering and enhanced crystallinity in the SVA film over the QLS one, Fig. 2.[22,11] In addition, in contrast to the QLS film of **1**, solvent annealing using DCB induces a dramatic blued-shift of the Q band from 655 nm for **1** in $CHCl_3$ solution to 642 nm for the SVA film, Fig. S6† , indicating the presence of a strong face-to-face intermolecular stacking interaction and formation of *H*–aggregates between the π-conjugated triple-decker molecules.[19,23] As a consequence, simple solvent vapor annealing over the (Pc)Eu[Pc(ONh)$_8$]Eu[Pc(ONh)$_8$] QLS films not only induces significantly improvement over the molecular packing and ordering as well as the film-crystallinity but also achieves the successful fine controlling over the aggregation mode from *J*-type in the QLS films to *H*-type in the SVA films. The strong intramolecular–stacking in the triple-decker molecule together with intense intermolecular face-to-face interaction in the *H*–aggregates of the SVA film is believed to provide the electrons (or holes) with an extensive area for delocalization.[24]

As exemplified in Fig. 3 and Table S3†, in air the OFET devices fabricated from the SVA films of **1** on the HMDS-treated SiO_2/Si substrates with a bottom-gate top-contact configuration also showed typically ambipolar (both *p*- and *n*-channel) but enhanced performance in comparison with the QLS film counterparts as exemplified by the good current on/off ratio as high as 10^6. In particular, these devices present the high and balanced carrier mobilities of 1.71 cm^2 V^{-1} s^{-1} for holes (at V_{ds}= –20 V) and 1.25 cm^2 V^{-1} s^{-1} for electrons (at V_{ds}= 20 V), Fig. 3 and Table S3†. It should also be pointed out that among the totally examined 32 OFETs, over 70% devices exhibit carrier mobilities over 1 cm^2 V^{-1} s^{-1} with the average value for electrons of 1.25 ± 0.1 cm^2 V^{-1} s^{-1} and for holes of 1.75 ± 0.25 cm^2 V^{-1} s^{-1}, respectively, Fig. S9†.To the best of our knowledge, this result represents the ambipolar performance in terms of the highest carrier mobility value simultaneously for holes and electrons and in particular the balance between them among the solution-processed small-molecule single-component-based OFET devices under ambient conditions.[5,23] Nevertheless, even after 2 months stored under ambient conditions, the devices fabricated from the SVA films of this triple-decker compound still exhibit high and

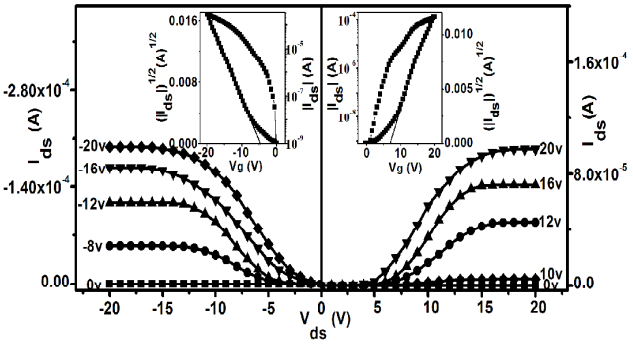

Fig. 3 Output characteristics (I_{ds} versus V_{ds}) and (inserts) transfer characteristics ($|I_{ds}|^{1/2}$ versus V_G) of ambipolar OFET device based on the SVA film of **1** deposited on HMDS-treated SiO_2/Si (300 nm) substrate with Au top contacts measured in air.

balanced electron and hole mobilities in the order of 1.0 $cm^2 V^{-1} s^{-1}$ (μ_h=1.11 $cm^2 V^{-1} s^{-1}$ and μ_e=1.04 $cm^2 V^{-1} s^{-1}$) with the current on/off ratio remaining unchanged for both *n*- and *p*-channel operations, Fig. S10† and Table S3†, indicating the good stability of the devices in air. It is worth noting that in the low source-drain biased voltage, the contact effect was observed for not only the electron but also the hole transport in the present work although almost no Mott–Schottky barrier exists for the hole injection due to the good matching between the HOMO (–5.07 eV) of (Pc)Eu[Pc(ONh$_8$]Eu[Pc(ONh$_8$] and the Fermi level of the Au electrode (–5.1 eV). As a result, the contact effect observed for both electron and hole transport in the low source-drain voltage range should be attributed mainly to the injection barriers from charge carrier trap states within the solution-based organic semiconductor film and at the organic semiconductor-metal interface.[25] However, it is should be pointed out again that despite the relatively large injection barriers, surprisingly efficient electron and hole injection from gold into the semiconductor layer still becomes possible along with the increase in the source-drain voltage, resulting in high carrier mobilities for both holes and electrons that can be extracted from the saturation regime. This result seems to indicate that the transfer and output characteristics for the ambipolar triple-decker organic semiconductor have not been affected by the contact resistance in the saturation regime since the gate field applied induces additional charges to fill the deep trap states, Fig. 3, which in turn helps the hole and electron injection from the gold electrodes to the organic semiconducting layer.

As can be expected, significant improvement in particular in terms of the balance between the threshold voltages (V_T) for holes and electrons has also been achieved after solvent annealing of the QLS films of **1**. The quite low and balanced threshold voltages for holes and electrons, –5 and +9 V, respectively, obtained for the SVA film-based OFET devices of **1**, in combination with the high charge mobilities and good on/off ratio, ensure the application potential of this ambipolar organic semiconductor with air stable nature in low-power nano-electronics.[26] In addition, the operating voltage range applied decreases from 0 ~ ±80 V for QLS film-based OFETs to 0 ~ ±20 V for the SVA film-based devices, indicating the effect of the molecular alignment and ordering improvement by solvent-vapor annealing on the device behavior. Nevertheless, in the present case the high and balanced carrier mobilities for holes and electrons have been actually recorded at both quite smaller source-drain voltage range (V_{ds} = 0 ~ ±20 V) and gate voltage range (Vg = 0 ~ ±20 V) in comparison with most organic thin film transistors usually with the larger V_{ds} and V_g range than 0 ~ ±20 V reported previously.[27] Furthermore, both the output and transfer curves for the (Pc)Eu[Pc(ONh$_8$]Eu[Pc(ONh$_8$] ambipolar OFET devices at low gate bias do not show the current increase in a superlinear manner at high drain bias, Figs. 3 and S7†, due likely to the considerably lower injection barrier simultaneously for holes and electrons,[28] ensuring their future practical applications. Actually, careful inspection over the OFET devices reported thus far reveals that in comparison with the single-polar OFET devices, ambipolar OFETs show much more examples with the superlinear feature observed in the output curves at gate bias of 0 V[29] due to the large carrier barrier for either holes and/or electrons because of the lack of simultaneously match for the work function of metal electrodes with the HOMO and/or LUMO level of ambipolar semiconductor.[25a,30] As a result, for the purpose of effectively eradicating the superlinear property of ambipolar OFET devices, various methods have been developed to lower the injection barrier simultaneously for holes and electrons, including varying the work function of the electrodes,[31] employing two-component organic heterostructure,[1,32] or utilizing a low bandgap organic semiconductor.[5a,33] In the present case, the HOMO level of (Pc)Eu[Pc(ONh$_8$]Eu[Pc(ONh$_8$] aligns well with the work function of gold electrodes, ensuring an ohmic contact for hole injection from gold into the semiconductor layer. More interestingly, despite the mismatch between the work function of Au electrode and the LUMO energy level of (Pc)Eu[Pc(ONh$_8$]Eu[Pc(ONh$_8$] at –4.00 eV (if this acted as the sole factor, an electron injection barrier as large as 1.1 eV in a zero-order vacuum alignment picture would be anticipated), an Ohmic-like contact for electron injection still becomes possible due to the formation of interface dipoles[34] at the Au/(Pc)Eu[Pc(ONh$_8$]Eu[Pc(ONh$_8$] interface, which also considerably lower the electron injection barrier, ensuring and rationalizing the observation of a non-superlinear transport also for electrons. This is in line with those observed for good ambipolar OFET devices reported previously.[31-34]

Conclusions

Briefly summarizing above, a simple solvent-vapor annealing approach using high boiling-point marginal solvent DCB over the QLS films fabricated from heteroleptic (Pc)Eu[Pc(ONh$_8$]Eu[Pc(ONh$_8$] with unsymmetrical triple-decker molecular structure and bringing peripheral slightly electron-withdrawing naphthoxy substituents led to more ordered molecular packing in the film, enabling the excellent ambipolar OFET device performance that has never been revealed for a small molecule single-component-based solution processed devices, with the high and balanced mobilities of 1.71 and 1.25 $cm^2 V^{-1} s^{-1}$, low threshold voltages of –5 and +9 V for holes and electrons, respectively, and high on/off ratios of 10^6. The present result will be helpful for the design and preparation of air-stable, high performance ambipolar OFET devices with potential application in the ultra-low-cost, large-area complementary integrated circuits through the combination of molecular design and interface engineering.

Acknowledgements

This work was financially supported by the National Key Basic Research Program of China (No. 2013CB933402 and 2012CB224801) and the National Natural Science Foundation of China (No. 21290174 and 21371073).

Notes and references

[a] *Shandong Provincial Key Laboratory of Fluorine Chemistry and Chemical Materials, School of Chemistry and Chemical Engineering, University of Jinan, Jinan 250022, China. E-mail: chm_chenyl@ujn.edu.cn; Fax: +86 (0)531 8973 6150*

[b] *Beijing Key Laboratory for Science and Application of Functional Molecular and Crystalline Materials, Department of Chemistry, University of Science and Technology Beijing, Beijing 100083, China.. E-mail: jianzhuang@ustb.edu.cn Fax: +86 (0)010 6233 2462*

†Electronic Supplementary Information (ESI) available: [Synthesis details, procedure of the film-preparation, structural characterization data and additional physical characterization data]. See DOI: 10.1039/c000000x/

1 A. Dodabalapur, H. Katz, L. Torsi and R. Haddon, *Science,* 1995, **269**, 1560.

2 (a) Y. Guo, G. Yu and Y. Liu, *Adv. Mater.,* 2010, **22**, 4427; (b) P. Sonar, S. P. Singh, Y. Li, M. S. Soh and A. Dodabalapur, *Adv. Mater.,*2010, **22**, 5409; (c) Y. Zhao, Y. Guo and Y. Liu, *Adv. Mater.,* 2013, **25**, 5372.

3 G. Guillaud, M. A. Sadoun, M. Maitrot, J. Simon and M. Bouvet, *Chem. Phys. Lett.,* 1990, **167**, 503.
4 (a) H. Dong, X. Fu, J. Liu, Z. Wang and W. Hu, *Adv. Mater.,* 2013, **25**, 6158; (b) J. Mei, Y. Diao, A. L. Appleton, L. Fang and Z Bao, *J. Am. Chem. Soc.,* 2013, **135**, 6724; (c) K. Walzer, B. Maennig, M. Pfeiffer and K. Leo, *Chem. Rev*., 2007, **107**, 1233; (d) M. Baldo, M. Thompson and S. Forrest, *Natur*e, 2000, **403**, 750.
5 (a) W. Wu, Y. Liu and D. Zhu, *Chem. Soc. Rev.,* 2010, **39**, 1489; (b) R. P. Ortiz, A. Facchetti and T. J. Marks, *Chem. Rev.,* 2010, **110**, 205.
6 (a) M. L. Tang, A. D. Reichardt, N. Miyaki, R. M. Stoltenberg and Z. Bao, *J. Am. Chem. Soc*., 2008, **130**, 6064; (b) N. Benson, M. Schidleja, C. Melzer, R. Schmechel and H. von Seggern, *Appl. Phys. Lett.,* 2006, **89**, 182105; (c) T. B. Singh, T. Meghdadi, S. Gunes, N. Marjanovic, G. Horowitz, P. Lang, S. Bauer and N. S. Sariciftci, *Adv. Mater.,* 2005, **17**, 2315.
7 (a) S. Z. Bisri, T. Takenobu, T. Takahashi and Y. Iwasa, *Appl. Phys. Lett.,* 2010, **96**, 183304; (b) M. Yamagishi, J. Takeya, Y. Tominari, Y. Nakazawa, T. Kuroda, S. Ikehata, M. Uno, T. Nishikawa and T. Kawase, *Appl. Phys. Lett.,* 2007, **90**, 182117.
8 Z. Liang, Q. Tang, R. Mao, D, Liu, J. Xu and Q. Miao, *Adv. Mater.,* 2011, **23**, 5514.
9 J. Kan, Y. Chen, D. Qi, Y. Liu and J. Jiang, *Adv. Mater.,* 2012, **24**, 1755.
10 X. Zhang and Y. Chen, *Inorg. Chem. Commun.,* 2014, **39**, 79.
11 D. Khim, K. Baeg, J. Kim, M. Kang, S. –H. Lee, Z. Chen, A. Facchetti, D.-Y. Kim and Y.-Y. Noh, *ACS Appl. Mater. Inter.,* 2013, **5**, 10745.
12 K. C. Dickey, J. E. Anthony and Y. L. Loo, *Adv. Mater.,* 2006, **18**, 1721.
13 D. Li, H. Wang, J. Kan, W. Lu, Y. Chen and J. Jiang, *Org. Electron*., 2013, **14**, 2582.
14 H. Usta, C. Risko, Z. Wang, H. Huang, M. K. Deliomeroglu, A. Zhukhovitskiy, A. Facchetti and T. J. Marks, *J. Am. Chem. Soc.,* 2009, **131**, 5586.
15 Y. Chen, M. Bouvet, T. Sizun, Y. Gao, C. Plassard, E. Lesniewska and J. Jiang, *Phys. Chem. Chem. Phys.,* 2010, **12**, 12851.
16 (a) J. F. Liu, K. Z. Yang and Z. H. Lu, *J. Am. Chem. Soc.,* 1997, **119**, 11061; (b) K. Xiao, Y. Liu, G. Yu and D. Zhu, *Appl. Phys. A,* 2003, **77**, 367; (c) T. Yamamoto, H. Kokubo, M. Kobashi and Y. Sakai, *Chem. Mater.,* 2004, **16**, 4616.
17 M. Yoneyama, M. Sugi, M. Saito, K. Ikegami, S. i. Kuroda and S. Iizima, *Jpn. J. Appl. Phys.,* 1986, **25**, 961.
18 K. Wang, D. Qi, H. Wang, W. Cao, W. Li and J. Jiang, *Chem.-Eur. J.,* 2012, **18**, 15948.
19 M. Kasha, H. Rawls and M. Ashraf El-Bayoumi, *Pure Appl. Chem.,* 1965, **11**, 371.
20 S. M. Sze, *Physics of Semiconductor Devices*, John Wiley &Sons, New York, 1981.
21 K. Balakrishnan, A. Datar, T. Naddo, J. Huang, R. Oitker, M. Yen, J. Zhao and L. Zang, *J. Am. Chem. Soc.,* 2006, **128**, 7390.
22 (a) L. Li, Q. Tang, H. Li, X. Yang,W. Hu, Y. Song, Z. Shuai, W. Xu, Y. Liu and D. Zhu, *Adv. Mater.,* 2007, **19**, 2613; (b) C. Di, K. Lu, L. Zhang, Y. Liu, Y. Guo,X. Sun, Y. Wen, G. Yu and D. Zhu, *Adv. Mater.,* 2010, **22**, 1273.
23 (a) P. Gao, D. Beckmann, H. N. Tsao, X. Feng, V. Enkelmann, M. Baumgarten, W. Pisula and K. Müllen, *Adv. Mater.,* 2009, **21**, 213; (b) G. Giri, E. Verploegen, S. C. Mannsfeld, S. Atahan-Evrenk, D. H. Kim, S. Y. Lee, H. A. Becerril, A. Aspuru-Guzik, M. F. Toney and Z. Bao, *Nature,* 2011, **480**, 504; (c) Y. Zhao, C. Di, X. Gao, Y. Hu, Y. Guo, L. Zhang, Y. Liu, J. Wang, W. Hu and D. Zhu, *Adv. Mater.,* 2011, **23**, 2448.
24 (a) S. Kim, T. K. An, J. Chen, I. Kang, S. H. Kang, D. S. Chung, C. E. Park, Y. –H. Kim and S. –K. Kwon, *Adv. Funct. Mater.,* 2011, **21**, 1616; (b) F. Garnier, *Acc. Chem. Res.,* 1999, **32**, 209; c) G. Nagarjuna, M. Baghgar, J. A. Labastide, D. D. Algaier, M. D. Barnes, D. Venkataraman, *ACS Nano.,* 2012, **6**, 10750.
25 (a) J. Zaumseil and H. Sirringhaus, *Chem. Rev.,* 2007, **107**, 1296; (b) K. P. Pernstich, S. Haas, D. Oberhoff, C. Goldmann, D. J. Gundlach, B. Batlogg, A. N. Rashid and G. Schitter, *J. Appl. Phys.,* 2004, **96**, 6431; (c) J. H. Kim, S. W. Yun, B.-K. An, Y. D. Han, S.-J. Yoon, J. Joo and S. Y. Park, *Adv. Mater.,* 2013, **25**, 719.
26 (a) H. Klauk, U. Zschieschang, J. Pflaum and M. Halik, *Nature*, 2007, **445**, 745; (b) M. Halik, H. Klauk, U. Zschieschang, G. Schmid, C. Dehm, M. Schütz, S. Maisch, F. Effenberger, M. Brunnbauer and F. Stellacci, *Nature,* 2004, **431**, 963.
27 (a) A. L. Briseno, S. C. B. Mannsfeld, C. Reese, J. M. Hancock, Y. Xiong, S. A. Jenekhe, Z. Bao and Y. Xia, *Nano Lett.,* 2007, **7**, 2847; (b) J. A. Lim, H. S. Lee, W. H. Lee and K. Cho, *Adv. Funct. Mater.,* 2009, **19**, 1515; (c) H. Chen, Y. Guo, G. Yu, Y. Zhao, J. Zhang, D. Gao, H. Liu and Y. Liu, *Adv. Mater.,* 2012, **24**, 4618; (d) K. N. N. Unni, A. K. Pandey, S. Alem and J.-M. Nunzi, *Chem. Phys. Lett.,* 2006, **421**, 554.
28 (a) S. Z. Bisri, C. Piliego, J. Gao and M. A. Loi, *Adv. Mater.,* 2014, **26**, 1176; (b) J. Zaumseil, C. L. Donley, J.-S. Kim, R. H. Friend and H. Sirringhaus, *Adv. Mater.,* 2006, **18**, 2708; (c) E. J. Meijer, D. M. de Leeuw, S. Setayesh, E. van Veenendaal, B. -H. Huisman, P. W. M. Blom, J. C. Hummelen, U. Scherf and T. M. Klapwijk, *Nat. Mater.,* 2003, **2**, 678.
29 (a) T. Lei, J. Dou, Z. Ma, C. Liu, J. Wang and J. Pei, *Chem. Sci.,* 2013, **4**, 2447; (b) T. D. Anthopoulos, S. Setayesh, E. Smits, M. Cölle, E. Cantatore, B. de Boer, P. W. M. Blom and D. M. de Leeuw, *Adv. Mater.,* 2006, **18**, 1900.
30 (a) L.-L. Chua, J. Zaumseil, J.-F. Chang, E. C.-W. Ou, P. K.-H. Ho, H. Sirringhaus and R. H. Friend, *Nature,* 2005, **434**, 194; (b) T. D. Anthopoulos, D. M.de Leeuw, E. Cantatore, P. van't Hof, J. Alma and J. C. Hummelen, *J. Appl. Phys.,* 2005, **98**, 054503; (c) B. H. Hamadani and D. Natelson, *Appl. Phys. Lett.,* 2004, **84**, 443.
31 (a) T. Yamamoto, T. Yasuda, Y. Sakai and S. Aramaki, *Macromol. Rapid Commun.,* 2005, **26**, 1214; (b) R. Schmechel, M. Ahles and H. von Seggern, *J. Appl. Phys.,* 2005, **98**, 084511; (c) C. L. Song, C. B. Ma, F. Yang, W. J. Zeng, H. L. Zhang and X. Gong, *Org. lett.,* 2011, **13**, 2880.
32 (a) M. Cavallini, P. D'Angelo, V. V. Criado, D. Gentili, A. Shehu, F. Leonardi, S. Milita, F. Liscio and F. Biscarini, *Adv. Mater.,* 2011, **23**, 5091; (b) P. Cosseddu, A. Bonfiglio, I. Salzmann, J. P. Rabe and N. Koch, *Org. Electron.,* 2008, **9**, 191.
33 (a) J. M. Mativetsky, M. Kastler, R. C. Savage, D. Gentilini, M. Palma, W. Pisula, K. Müllen, and P. Samorí, *Adv. Funct. Mater.,* 2009, **19**, 2486; (b) J. Locklin, K. Shinbo, Ken Onishi, F. Kaneko, Z. Bao and R. C. Advincula, *Chem. Mater.,* 2003, **15**, 1404; (c) C. Liu, Z. Liu, H. T. Lemke, H. N. Tsao, R. C. G. Naber, Y. Li, K. Banger,

K. Müllen, M. M. Nielsen and H. Sirringhaus, *Chem. Mater.,* 2010, **22**, 2120.

34 (a) S. C. Veenstra, A. Heeres, G. Hadziioannou, G. A. Sawatzky and H. T. Jonkman, *Appl. Phys. A,* 2002, **75**, 661; (b) D. J. Gundlach, L. Zhou, J. A. Nichols, T. N. Jackson, P. V. Necliudov and M. S. Shur, *J. Appl. Phys.,* 2006, **100**, 024509.

